Journal of Earth Science, *Vol. 32*, *No. 6*, *p. 1445–1453*, *December 2021* *ISSN 1674-487X*
Printed in China
https://doi.org/10.1007/s12583-020-1358-y

Melt-Lithosphere Interaction Controlled Compositional Variations in Mafic Dikes from Fujian Province, Southeastern China

Zhuliang Lei[1], **Gang Zeng***[1], **Jianqiang Liu***[2], **Xiaojun Wang**[1], **Lihui Chen**[1], **Xiaoyu Zhang**[1], **Jinhua Shi**[1]

1. *State Key Laboratory for Mineral Deposits Research*, *School of Earth Sciences and Engineering*, *Nanjing University*, *Nanjing* 210023, *China*
2. *Institute of Marine Geology*, *College of Oceanography*, *Hohai University*, *Nanjing* 210098, *China*

Zhuliang Lei: https://orcid.org/0000-0002-8739-8060; Gang Zeng: https://orcid.org/0000-0002-2198-3646; Jianqiang Liu: https://orcid.org/0000-0002-3828-0189

ABSTRACT: Late Mesozoic magmatism in southeastern China has been widely considered to be related to the subduction of the Paleo-Pacific Plate. However, it remains controversial whether mafic rocks are derived from the lithosphere or the asthenosphere. Here we present a comprehensive study on mafic dikes from Fujian Province in southeastern China, aiming to understand their source. Two types of mafic rocks have been recognized based on their trace-element features. Type-I rocks show arc-like trace-elemental characteristics, while type-II rocks are distinguished by their relatively flat patterns in primitive-mantle-normalized trace-element diagram. Despite such differences between two types of rocks, these mafic dikes show two trends in the plots of $^{87}Sr/^{86}Sr_{(i)}$ versus La/Nb, which can be explained by the influences of crustal contamination and melt-lithospheric mantle interaction, respectively. $^{87}Sr/^{86}Sr_{(i)}$, La/Nb, Sr/Y and Zr/Y ratios of type-I rocks are significantly correlated to the thickness of the underlying lithosphere, and the signals of lithosphere are clearer with increasing lithospheric thickness. This highlights the important influences of melt-lithosphere interaction during their formation. Such observations also indicate that these mafic rocks are more likely to have been originated from the asthenosphere rather than the lithospheric mantle.

KEY WORDS: mafic dike, lithospheric mantle, asthenosphere, melt-lithosphere interaction, southeastern China.

0 INTRODUCTION

Widespread Late Mesozoic magmatism in southeastern China is generally related to the subduction of the Paleo-Pacific Plate (Wang et al., 2018; He and Xu, 2012; Li and Li, 2007; Zhou et al., 2006; Zhou and Li, 2000; Jahn et al., 1990; Jahn, 1974). As the products of subduction, most of the Mesozoic mafic rocks in southeastern China exhibit arc-like features, especially marked by the enriched large ion lithophile elements (LILEs) and light rare earth elements (LREEs) and relative depleted high field strength elements (HFSEs). However, the magma source of these mafic rocks (including basalts and diabases) is still controversial. In the past few decades, these mafic magmas are generally suggested to have been originated from a fluid/melt-metasomatized lithospheric mantle, and their source lithology is suggested to be peridotite, the most common lithology in the upper mantle (Zhao et al., 2007, 2004; Wang et al., 2003). However, recent studies on Late Mesozoic basalts suggested that their source lithology should be pyroxenite rather than peridotite (Jia et al., 2020; Zeng et al., 2016), and such basaltic melts with arc-like geochemical characteristics are likely to be derived from deep asthenospheric source rather than the lithospheric mantle (Zhang et al., 2019; Meng et al., 2012; Chen et al., 2008). In fact, previous studies on basalts in oceanic (Niu et al., 2011; Humphreys and Niu, 2009) and continental setting (Davies et al., 2015) generally suggested the asthenosphere as their source, and the lithosphere is involved to control the melting depth via its thickness, called "Lid Effect", which can indirectly affect the chemical compositions of these basalts. Alternatively, during ascent, the asthenosphere-derived initial melts have the chance to interact with the lithosphere, and therefore their chemical compositions can be modified directly (Zhang et al., 2017; Zeng et al., 2013). In this case, lithospheric thickness becomes an important factor to affect the interaction degree (Liu et al., 2016). Therefore, the source of Mesozoic mafic rocks and the potential role of lithosphere during their formation still need to be assessed.

Late Mesozoic mafic dikes are well developed in Fujian Province, southeastern China. Previous studies focused on the

*Corresponding authors: zgang@nju.edu.cn; liujq@hhu.edu.cn

Manuscript received February 20, 2020.
Manuscript accepted May 18, 2020.

Lei, Z. L., Zeng, G., Liu, J. Q., et al., 2021. Melt-Lithosphere Interaction Controlled Compositional Variations in Mafic Dikes from Fujian Province, Southeastern China. *Journal of Earth Science*, 32(6): 1445–1453. https://doi.org/10.1007/s12583-020-1358-y. http://en.earth-science.net

mafic dike swarms in the coastal region, here we select two mafic dikes (namely Bali and Panting), which are distributed in the area west of the Zhenghe-Dapu fault, to conduct a comprehensive petrological and geochemical study. We divide Late Mesozoic mafic dikes in Fujian Province into four groups based on underlying lithospheric thickness to examine how they evolved with different lithospheric thickness.

1 GEOLOGICAL BACKGROUND AND PETROGRAPHY

The South China Block (SCB) consists of the Yangtze Block in the west and the Cathaysia Block in the east, which amalgamated along a Neoproterozoic collision belt (Chen and Jahn, 1998). The Fujian Province is located in the eastern part of the SCB, and there are two large-scale NNE-SSW-trending faults: the Changle-Nan'ao and the Zhenghe-Dapu fault. The Fujian Province is subdivided into three tectonic belts (from east to west) by these two faults: the Pingtan-Dongshan metamorphic belt, the Yanshanian magmatic belt, and an Early Paleozoic fold belt (Chen et al., 2002) (Fig. 1). Mesozoic magmatic rocks are widely distributed in the southeastern China, over 90% of which are granitoids and equivalent volcanic rocks with minor mafic rocks such as basalts and diabases (Zhou et al., 2006). Mesozoic mafic dikes are well developed in the Fujian Province, especially in the coastal region. Geophysical studies show that the lithospheric thickness decreases from the west to the east in eastern China (Shen et al., 2019; Feng et al., 2010). Moreover, Wan et al. (1987) considered that the thickness of the lithosphere in eastern Fujian was thinner based on the research of silica heat flow in Fujian, so we speculate that the lithospheric thickness beneath the Fujian Province increases gradually from the coast area to the interior.

In this study, we sampled two mafic dikes located in the western Fujian Province (namely Bali and Panting). The mafic dikes from Bali are hornblende gabbros, consisting mainly of plagioclase (62%), hornblende (20%), pyroxene (<15%) and accessory minerals such as magnetite. Plagioclase is euhedral to subhedral in shape and hornblende is subhedral to anhedral, and some of the hornblende and pyroxene have been partially chloritized (Figs. S1a, S1b). Previous studies obtained a whole-rock K-Ar age of 79.3±1.3 Ma (Zhang, 2006). The Panting diabase dikes are composed chiefly of plagioclase (80%) and pyroxene (20%). Plagioclase is generally euhedral to subhedral, pyroxene is anhedral, which are filled mainly in the triangular frame made up of plagioclase. Parts of the pyroxenes have been chloritized and plagioclases have been kaolinizated (Figs. S1c, S1d). Previous whole-rock K-Ar dating results yielded emplacement ages ranging from 99.8±3.0 to 117.9±3.5 Ma (Zhao, 2004).

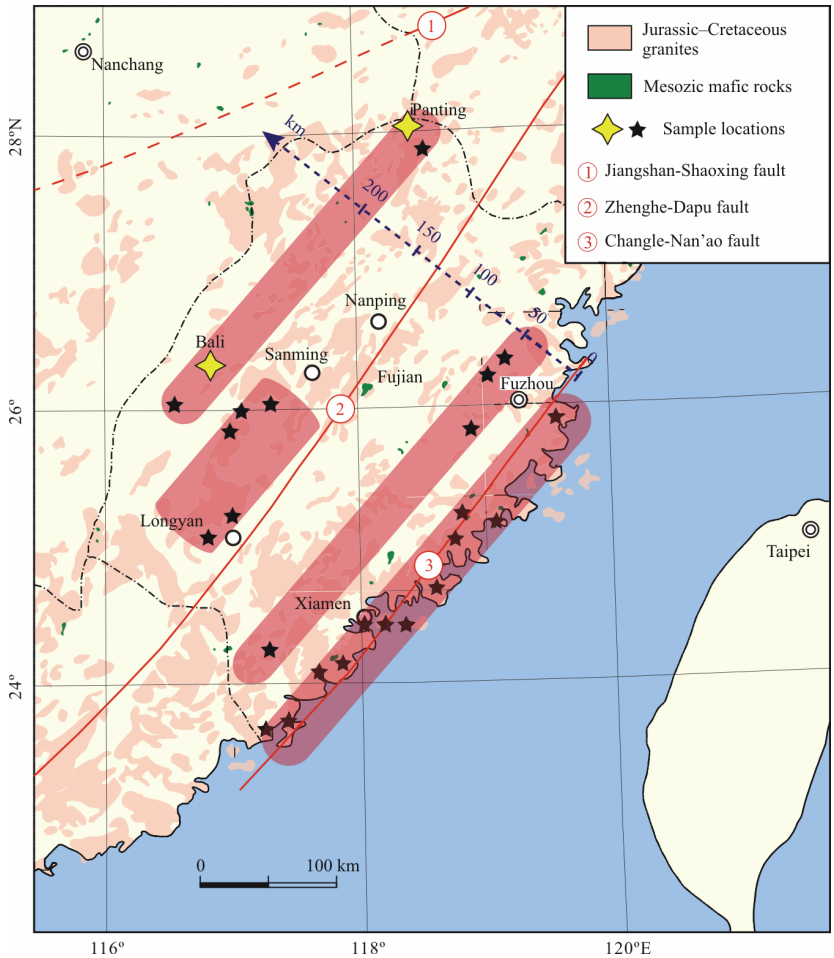

Figure 1. Simplified geological map of Fujian Province showing the distribution of Mesozoic granites and mafic rocks (modified after Zhou et al., 2006). The sampling locations in this study are shown as four-angle stars, literature sample locations are shown as pentagrams (Dong et al., 2011; Qin et al., 2010; Chen et al., 2008; Yang, 2008; Zhang, 2006; Zhao, 2004).

2 ANALYTICAL METHODS

The samples for whole-rock geochemical analyses were firstly crushed into gravel-size chips. Clean chips were then powdered to 200 mesh for chemical analysis in a corundum mill. Major and trace element compositions, as well as Sr, Nd, Hf isotopes were measured for all samples.

Measurements of whole-rock major elements were performed by using a Thermo Scientific ARL 9900 X-ray fluorescence spectrometer at the State Key Laboratory for Mineral Deposits Research, Nanjing University, China. The measured values of diverse rock reference materials (BHVO-2 and BCR-2) indicate that the uncertainties are less than ±3% for elements Si, Ti, Al, Fe, Mn, Mg, Ca, K and P and less than ±6% for Na (Table S1).

Trace element concentrations of the samples were determined by using an ELAN 6100DRC inductively coupled plasma mass spectrometer (ICP-MS) after acid digestion (HF+HNO_3) in teflon beakers at the Department of Geology, Northwest University, China. The analytical errors are better than 5% for Sc, V, Co, Sr, Y, Zr, Nb, Ba, Hf, Ta, Pb, Th, U and rare earth elements (REE), and 7% for Cr, Ni, Rb and Cs, based on repetitive analyses of USGS rock standards (BHVO-2, BCR-2 and AGV-2; reference data are from Jochum et al. (2016)). The results of the analyses of these reference materials and blanks are summarized in Table S2.

Isotopic compositions of Sr, Nd and Hf were measured at the State Key Laboratory for Mineral Deposits Research, Nanjing University. Sample powders (~200 mg) were weighed in teflon capsules and then dissolved in distilled HF-HNO_3-$HClO_4$ (1.5 mL-1 mL-60 μL) at 130 ºC for more than 36 h. The chemical procedure of Sr, Nd, and Hf separation from natural rock samples consists of two steps (Lei et al., 2019). In the first step, a column filled with Eichrom Ln Spec+Sr-Spec+cation exchange resin (Bio-Rad AG50W-X8) was used to separate Sr, REE and HFSE. 5 mL of 7 mol/L HNO_3+1 mol/L HF was added to the column to elute REE and HFSE, and 5 mL of 0.05 mol/L HNO_3 was added to the column as a Sr elution. In the second step, Hf and Nd were separated by a column filled with Eichrom Ln Spec resins. 6 mL of 0.25 mol/L HCl was added to the column as a Nd elution, and 2 mL of 2 mol/L HF was added to the column as a Hf elution.

Strontium isotopic analyses were performed by using a Finnigan MAT Triton Tl thermal ionization mass spectrometry (TIMS), while Nd and Hf isotopic compositions were obtained by using a Neptune plus (Thermal Fisher Scientific) multi-collector inductively coupled plasma mass spectrometer (MC-ICP-MS). The Sr, Nd and Hf isotopic data were corrected for mass fractionation bias using $^{86}Sr/^{88}Sr$=0.119 4, $^{146}Nd/^{144}Nd$=0.721 9, and $^{179}Hf/^{177}Hf$=0.732 5, respectively. During the analyses, the measured Sr, Nd and Hf isotopic ratios were corrected for instrumental drift by reference to replicate analyses of standards NIST-987, JNdi-1 and JMC-475, respectively. Measured average $^{87}Sr/^{86}Sr$ values for NIST-987, $^{143}Nd/^{144}Nd$ values for JNdi-1, and $^{176}Hf/^{177}Hf$ values for JMC-475 were 0.710 228±0.000 011 (2SD, n=7), 0.512 101±0.000 026 (2SD, n=5) and 0.282 149±0.000 028 (2SD, n=12), respectively. During the whole-rock Sr-Nd-Hf analyses, the USGS reference materials (BHVO-2, AGV-2 and BCR-2) were analyzed as unknowns to monitor accuracy of analytical procedures, and their measured values are reported in Table S3. Measured values for these USGS reference materials show good agreement with recommended reference values.

3 GEOCHEMICAL RESULTS

3.1 Bulk-Rock Major and Trace Elements

The analytical results for major oxides (wt.%) and trace element (ppm) compositions of mafic dikes from Fujian Province are presented in Table S4. These mafic dikes show large variations in SiO_2 (43.9 wt.%–51.5 wt.%), TiO_2 (0.9 wt.%–3.4 wt.%), Al_2O_3 (13.6 wt.%–16.0 wt.%), $Fe_2O_3^T$ (8.6 wt.%–15.2 wt.%), MnO (0.1 wt.%–0.3 wt.%), MgO (3.6 wt.%–10.0 wt.%), CaO (8.2 wt.%–10.9 wt.%), and total alkalis (Na_2O+K_2O=3.1 wt.%–6.2 wt.%) contents. According to the nomenclature of Le Bas et al. (1986), they are classified as basalts and basaltic andesites, with minor samples plotting into the area of trachybasalts and trachyandesites (Fig. S2). Compared to the Bali mafic dikes, samples from Panting have generally higher TiO_2 and MnO contents, and lower MgO, Cr and Ni contents (Fig. 2). Loss on ignition (LOI) values of all samples vary from 2.0 wt.% to 5.0 wt.%.

In the primitive-mantle-normalized trace element spider diagrams, samples from Bali show variable enrichment in LILEs (large ion lithophile elements, such as Rb, Ba and K) and light REEs, with depletion in HFSEs (high field strength elements, such as Nb, Ta and Ti) (Fig. 3a), as observed in most arc magmas (Pearce and Peate, 1995). Samples from Panting show depletion or no obvious anomaly in Th, U relative to Nb, Ta (Fig. 3b). There is no obvious Eu anomaly (Eu/Eu*=0.89–1.28) in both Bali and Panting mafic dikes.

Combined with other literature database (Dong et al., 2011; Qin et al., 2010; Chen et al., 2008; Yang, 2008; Zhang, 2006; Zhao, 2004), mafic dikes in Fujian Province can be divided into two types based on their diverse geochemistry. Type-I rocks (including Bali) are characterized by arc-like trace element geochemistry, and type-II rocks (including Panting) are distinguished by relatively flat primitive mantle-normalized patterns (Fig. 3).

3.2 Bulk-Rock Sr-Nd-Hf Isotopes

Whole-rock Sr-Nd-Hf isotopic compositions are presented in Table S5. The initial isotopic ratios ($^{87}Sr/^{86}Sr_{(i)}$, $\varepsilon_{Nd}(t)$ and $\varepsilon_{Hf}(t)$) are recalculated by using the whole-rock K-Ar ages of 110 Ma for Panting (obtained from Zhao (2004)) and 79 Ma for Bali (obtained from Zhang (2006)). Samples from Panting have $^{87}Sr/^{86}Sr_{(i)}$= 0.705 78–0.706 83, $\varepsilon_{Nd}(t)$= -3.5–0.7 and $\varepsilon_{Hf}(t)$= -4.1–4.0. Relative to Panting mafic dikes, samples from Bali show more enriched isotopic compositions ($^{87}Sr/^{86}Sr_{(i)}$=0.710 34–0.710 40, $\varepsilon_{Nd}(t)$= -5.1 and $\varepsilon_{Hf}(t)$= -9.5 to -9.3) (Fig. 4).

4 DISCUSSION

4.1 Alteration, Fractional Crystallization and Partial Melting

LOI is an important indicator to judge the potential influence of post-magmatic alteration. The range of LOI of the Fujian mafic dikes from 2.0 wt.% to 5.0 wt.%, together with weak chloritization and kaolinization of some minerals, such as pyroxene and plagioclase, indicates that they have experienced post-magmatic alteration. However, the good correlation between Zr (immobile incompatible element) and La (mobile incompatible element) (Fig. S3a) implies that the influence of post-magmatic alteration on these elements is limited. More-

over, there is no obvious correlation between LOI and Nb, La and $^{87}Sr/^{86}Sr_{(i)}$ (Figs. S3b–S3d), which also precludes a significant role of alteration.

The MgO content of mafic dikes in Fujian Province is positively correlated with the Cr and Ni contents (Fig. 2), indicating they have undergone the fractional crystallization of olivines. Samples with MgO<8 wt.% exhibit positive correlations between MgO and CaO/Al_2O_3 (Fig. 2f), indicating the fractionation of

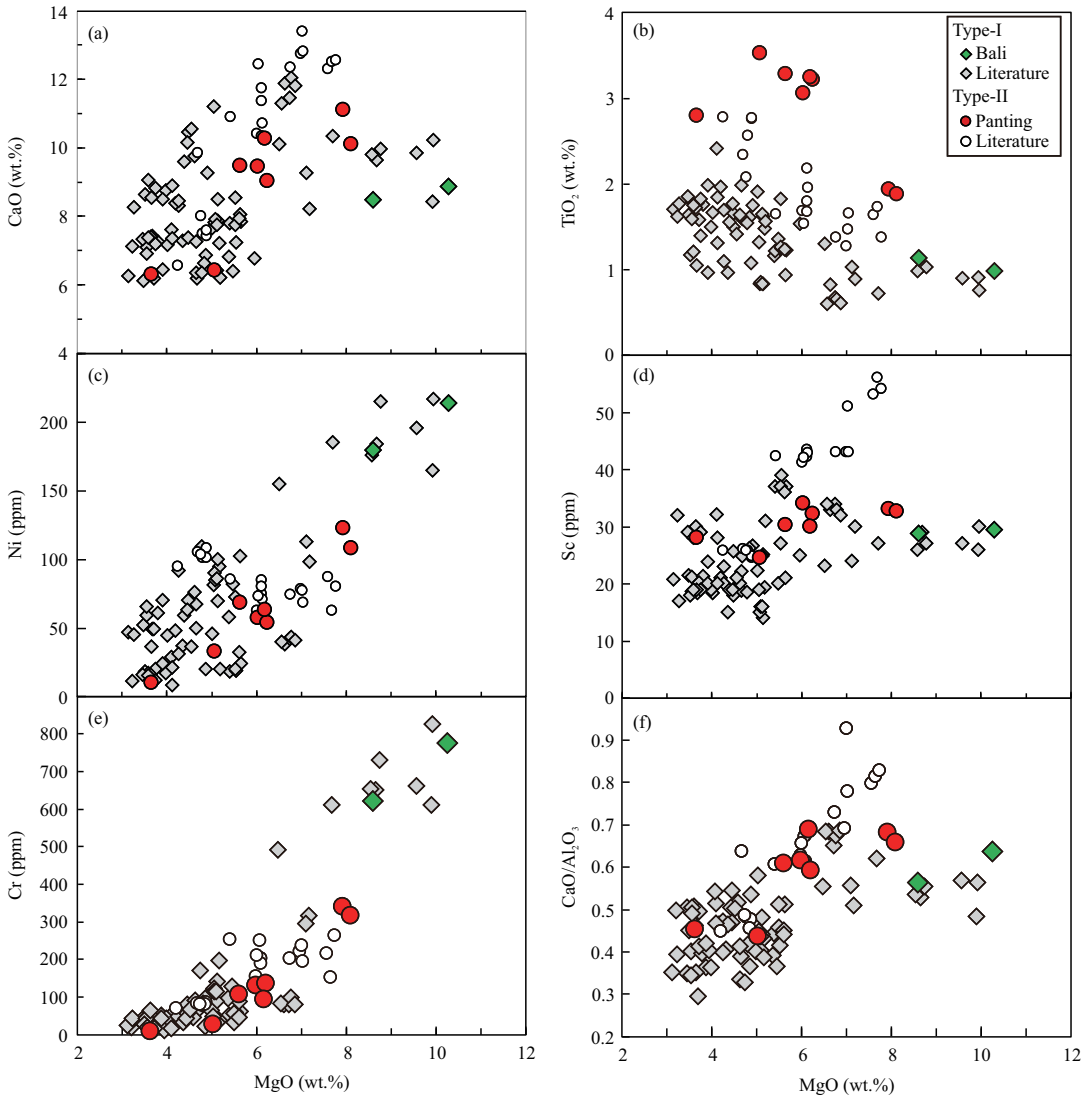

Figure 2. Variations of MgO versus CaO, TiO_2, Ni, Sc, Cr, and CaO/Al_2O_3 (a)–(f) for Late Mesozoic mafic dikes from Fujian Province. Literature data of mafic dikes are from Dong et al. (2011), Qin et al. (2010), Chen et al. (2008), Yang (2008), Zhang (2006) and Zhao (2004).

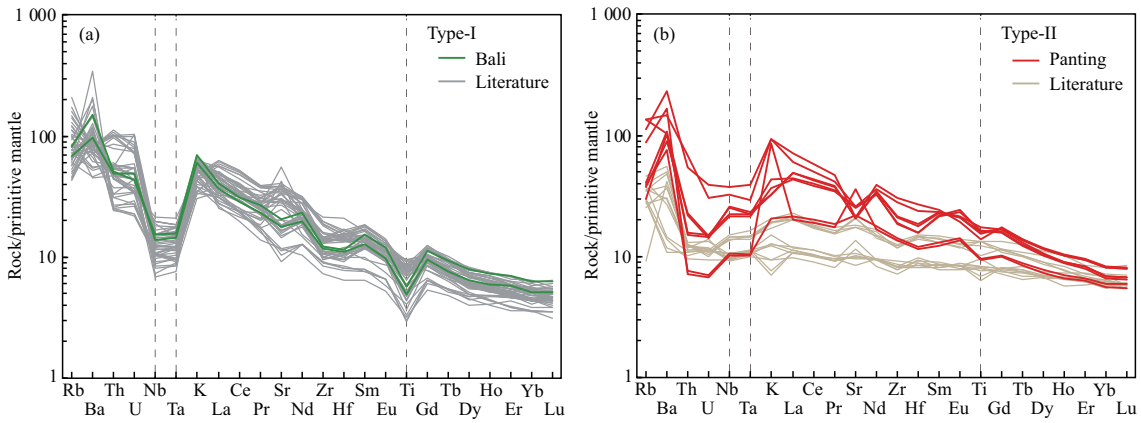

Figure 3. Primitive-mantle-normalized incompatible trace element diagrams for the Late Mesozoic mafic dikes from Fujian Province. The primitive mantle values are from McDonough and Sun (1995). Literature data sources are the same as in Fig. 2.

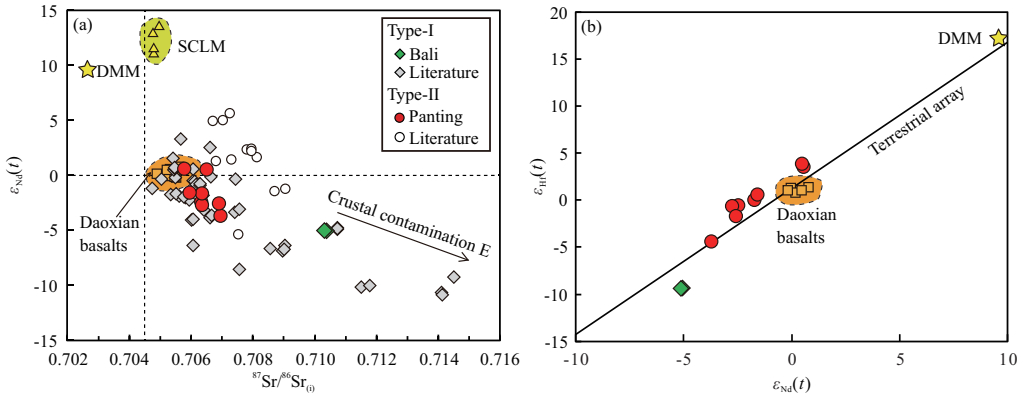

Figure 4. Variations in the Sr, Nd and Hf isotopic compositions of Late Mesozoic mafic dikes from Fujian Province. Data for SCLM are from Zhang et al. (2008). Data for Daoxian basalts are from Dai (2007). Data for depleted MORB mantle (DMM) are from Workman and Hart (2005). The terrestrial reference lines (ε_{Hf}=1.59×ε_{Nd}+1.28) are from Chauvel et al. (2008). Literature data sources are the same as in Fig. 2.

clinopyroxene. In addition, most samples do not show obvious Eu anomalies in the primitive-mantle-normalized incompatible element diagram (Fig. 3), suggesting the negligible influence of fractionation of plagioclase.

The La/Yb and Sm/Yb ratios of mafic dikes are controlled by both the mantle source and partial melting process. Most of type-II mafic dikes have lower La/Yb and Sm/Yb ratios than type-I samples (Fig. 5), which can be due to high degree melting of garnet-bearing peridotite/pyroxenite or partial melting of spinel-bearing peridotite. Type-I samples exhibit significantly high La/Yb and Sm/Yb ratios (Fig. 5). Such characteristics cannot be induced by the partial melting of spinel-bearing peridotite, and garnet is suggested to be present in the mantle source.

To exclude the potential effects of partial melting and fractionation of ferromagnesian minerals such as olivine and clinopyroxene, La/Nb ratios and Sr isotopic compositions of the Fujian mafic dikes are selected for discussion because La and Nb have comparable compatibility (Hofmann, 1988). The good correlations between Sr isotopes and La/Nb ratios indicate that the compositional variations of the Fujian mafic dikes are attributed to contamination process or source heterogeneity rather than partial melting or fractional crystallization process. Three end-members can be observed in the plots of La/Nb versus Sr (or Nd) isotopes (Figs. 6 and S4a), and for convenience, we define these end-members as component A, B and C, respectively. Because Hf isotopes have not been analyzed in previous studies, such phenomenon is not clear in the plots of La/Nb versus Hf isotopes (Fig. S4b). In the following section, we will discuss the potential candidate for each end-member.

4.2 Identification of Different Components

4.2.1 Component A: shallow crust materials

Component A shows extremely high $^{87}Sr/^{86}Sr_{(i)}$ ratio (>0.710) and low $\varepsilon_{Nd}(t)$ (< -7.5) (Figs. 6 and S4a). Such an isotopic characteristic has been suggested to be induced by crustal contamination (Zhao et al., 2007). More importantly, component A also shows high SiO_2 content (Fig. S5), which coincides with the trend of crustal contamination. Precambrian basement metamorphic rocks in western Fujian (Wan et al., 2007; Yu et al., 2003) show high $^{87}Sr/^{86}Sr$ ratios (>0.714) and low $\varepsilon_{Nd}(t)$ (< -8.8), and their variable La/Nb ratios (1.52–3.33) are similar with those of component

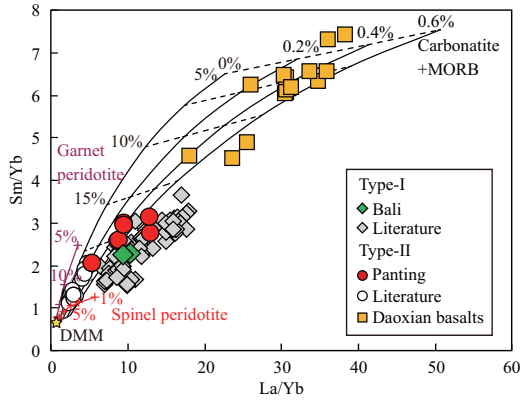

Figure 5. Variations in Sm/Yb versus La/Yb for Late Mesozoic mafic dikes from Fujian Province. Batch melting curves calculated for spinel peridotite, garnet peridotite and SiO_2-rich pyroxenite (with or without carbonatite: range from 0% to 0.6%), are also shown, details for parameters are listed in Table S6. Data for Daoxian basalts are from Dai (2007). Data for depleted MORB mantle (DMM) and average MORB are from Workman and Hart (2005) and Niu et al. (1999), respectively. The average values for carbonatites are based on data for oceanic magnesio-carbonatite from Cape Verdes (Hoernle et al., 2002). Literature data sources are the same as in Fig. 2.

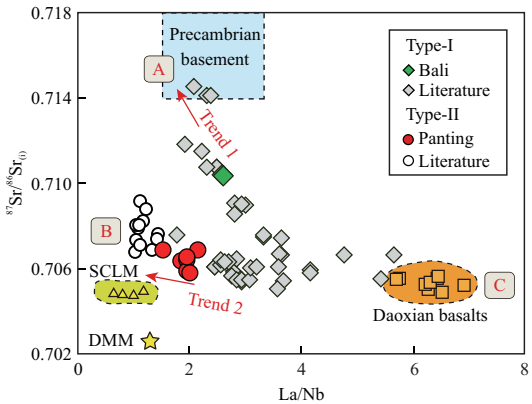

Figure 6. Variations in $^{87}Sr/^{86}Sr_{(i)}$ versus La/Nb values for Late Mesozoic mafic dikes from Fujian Province. Data for SCLM are from Zhang et al. (2008). Data for Daoxian basalts are from Dai (2007). Data for depleted MORB mantle (DMM) are from Workman and Hart (2005). Data for Precambrian basement metamorphic rocks in the South China Block are from Wan et al. (2007) and Yu et al. (2003). Literature data sources are the same as in Fig. 2.

A. The primary magma contaminated by such crustal materials can well explain the mixing trend 1 between components A and C (Fig. 6). Such a process is also expected to increase the SiO_2 contents of basaltic magmas. Therefore, we prefer to choose the crustal materials to represent component A. By comparison, mafic rocks involved in trend 2 show almost unchanged Sr isotopic compositions, which indicates the negligible influence of crustal contamination on these samples.

4.2.2 Component B: derived from the lithospheric mantle

Melts from component B show distinctive chemical signatures, including flat REE patterns (La/Yb=2.34–4.76), low La/Nb (1.05–1.24) and depleted Sr-Nd isotopic compositions ($^{87}Sr/^{86}Sr_{(i)}$=0.706–0.709, $\varepsilon_{Nd}(t)$=4.9–5.6) relative to those melts from component A (La/Yb>7, La/Nb=1.92–3.00, $^{87}Sr/^{86}Sr_{(i)}$> 0.710, $\varepsilon_{Nd}(t)$< -7.5). These signatures may result from partial melting, or may inherit from their mantle source.

The upper mantle is mainly composed of peridotite, which includes four major phases: olivine, orthopyroxene, clinopyroxene and an aluminous phase (i.e., spinel at lower pressure and garnet at higher pressure). REE partition coefficients differ markedly from garnet to spinel peridotites because the heavy REEs show strong affinity with garnet but are largely incompatible in spinel (Halliday et al., 1995; McKenzie and O'Nions, 1991). The flat REE pattern of component B-derived melts indicates that spinel rather than garnet is the residual mineral in the mantle source during partial melting. In general, the spinel-garnet phase transition in mantle peridotites occurs at the depth interval of 55–70 km in the upper mantle of eastern China (Fan et al., 1997). Because lithospheric thickness beneath eastern China is about 100 km (An and Shi, 2006), we inferred that component B should be located in the lithospheric mantle. Spinel lherzolite xenoliths hosted in the Ningyuan Mesozoic basalts (151–131 Ma) show nearly flat REE patterns without obviously HFSE anomalies (La/Nb=0.65–1.19), slightly higher Sr isotopic compositions and depleted Nd isotopic compositions (Zhang et al., 2008). All these characteristics coincide with the properties of component B, supporting our proposal of lithospheric mantle genesis for component B.

4.2.3 Component C: derived from the asthenosphere

Compared to component B, which has been suggested to be located in the shallow spinel-bearing lithospheric mantle, component C has more depleted Sr isotopes and higher LREE/HREE ratios (La/Yb>17). Garnet-bearing peridotite or pyroxenite, rather than spinel peridotite, is the possible source lithologies for this component, because HREEs are compatible in garnet and the high LREE/HREE ratios of this component requires garnet residual in their source (Halliday et al., 1995). The quantitative geochemical calculation also supports this inference (Fig. 5). Therefore, we argue a deeper source of component C than that of component B.

Furthermore, component C is characterized by slightly higher Sr isotopic ratios to DMM and arc-like trace element geochemistry, including the enrichment in LILEs and LREEs and depletion in HFSEs (such as Nb, Ta and Ti). These characteristics are generally explained by a source metasomatized by the subduction-released fluids/melts, and such metasomatized peridotite has been proposed to present either in the lithospheric mantle (Zhao et al., 2007, 2004; Wang et al., 2003) or in the asthenosphere (Zhang et al., 2019; Meng et al., 2012; Chen et al., 2008). Alternatively, via the identification of source lithologies, garnet pyroxenite, transformed from the subducted slab (Herzberg, 2011; Sobolev et al., 2007), has been involved to play an important role in the formation of these Mesozoic mafic rocks (Jia et al., 2020; Zeng et al., 2016). These studies highlight the direct participation of such mafic lithologies in the generation of mantle-derived, mafic magma, and do not stress the necessity of specific metasomatism. Additionally, Daoxian basalts, which have the highest La/Nb ratios among these mafic rocks (Fig. 6), show significantly negative anomalies of Zr, Hf, Nb, Ta, and Ti in the primitive-mantle-normalized incompatible element diagram (Zeng et al., 2016). The negative Zr, Hf and Ti anomalies observed in the basalts are generally explained by the involvement of carbonated component since carbonatite is enriched in incompatible elements except for Zr, Hf, and Ti (Zeng et al., 2010), and carbonated eclogite is therefore suggested to be the potential source lithology (Zeng et al., 2016). Melting of carbonated eclogite can also explain negative Nb and Ta anomalies because of the presence of rutile as a residual phase, in which these elements are compatible (Foley et al., 2000). All these mafic lithologies with or without carbonated components can melt much deeper than the peridotite in the upper mantle (Litasov and Ohtani, 2010; Dasgupta et al., 2004; Yasuda et al., 1994), and therefore these pyroxenites are more likely to present in the asthenosphere.

4.3 Melt-Rock Interaction and Compositional Evolution of Melts

Via the identification of three components mentioned above, two trends observed in the plots of La/Nb vs. Sr-Nd isotopic ratios (Figs. 6 and S4) might be explained by two potential geological process: crustal contamination (trend 1) and melt-lithospheric mantle interaction (trend 2). If such model is true, the thickness of lithosphere should be an important factor to affect the degree of interaction and the compositions of mafic rocks. To investigate the potential effects of varying lithospheric thickness on melt compositions, we divided the samples into four groups based on the distance to the Changle-Nan'ao fault (Fig. 1, Table S7). The thickness of lithosphere increases gradually from the Fujian coast area to the interior (Shen et al., 2019; Feng et al., 2010; Wan et al., 1987). With increasing thickness of lithosphere, type-I rocks become more enriched in the Sr isotopic compositions, while the La/Nb, Sr/Y and Zr/Y ratios decrease from the coast area to the interior (Fig. 7), suggesting the influence of lithosphere on rock chemistry. In general, the partial melting degree is suggested to decrease with increased thickness of lithosphere. However, in this condition, La/Nb, Sr/Y and Zr/Y ratios of melts also increase with increased thickness of lithosphere, which seems to be inconsistent with the trends observed in Fig. 7. More importantly, partial melting process cannot change the isotopic compositions of mafic melts. The other possible explanation is that these elemental ratios are modified by the melt-lithosphere interaction. Because of the disequilibrium in chemistry, melts from deeper mantle would interact with surrounding lithosphere when they passed through the lithosphere. As mentioned before, carbonated

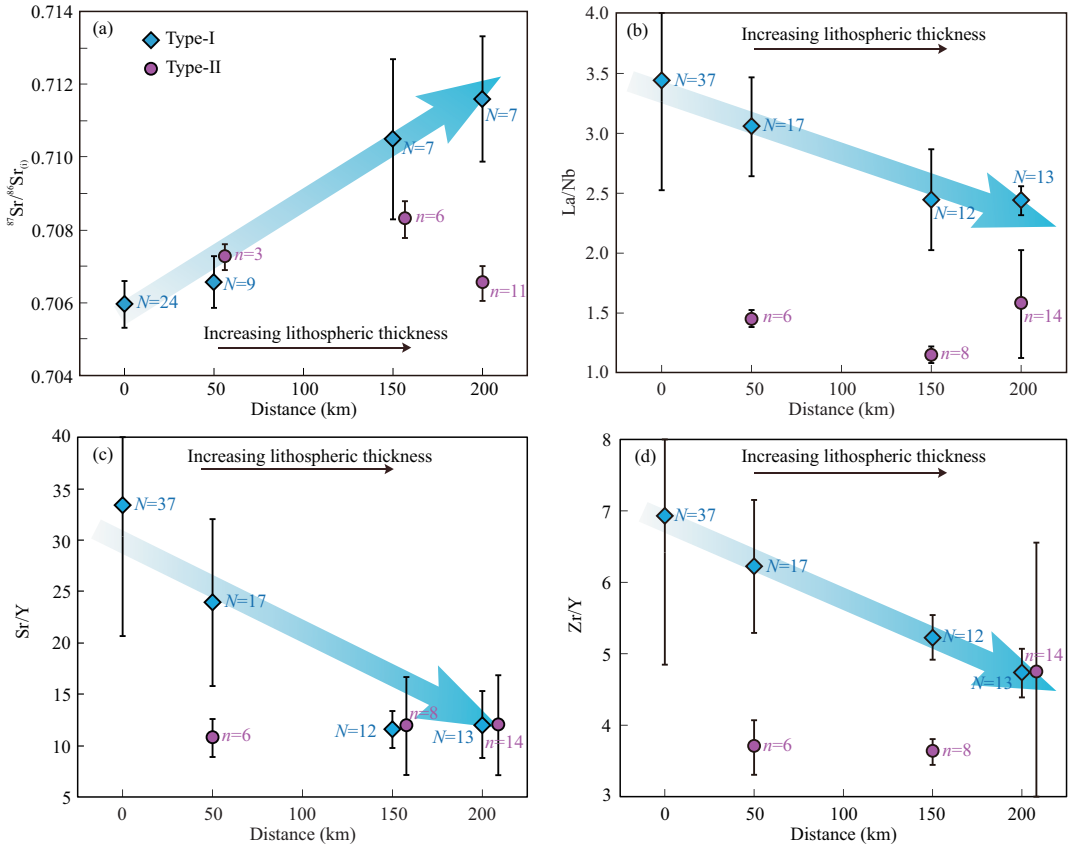

Figure 7. Variations of average (a) $^{87}Sr/^{86}Sr_{(i)}$, (b) La/Nb, (c) Sr/Y, and (d) Zr/Y with increasing lithospheric thickness for Late Mesozoic mafic dikes from Fujian Province. Abscissa represents the distance from sample location to the Changle-Nan'ao fault as shown in Fig. 1, details are listed in Table S7. *N* (*n*) represents the number of samples averaged for geochemical compositions and the error bars correspond to 1 standard error (1 SE) of the mean.

eclogite is suggested to be the potential source lithology of type-I rocks, which is suggested to have higher La/Nb, Sr/Y, Zr/Y and lower Sr isotopic compositions (represented by the Daoxain basalts: La/Nb=4.44–6.91, Sr/Y=17.8–60.9, Zr/Y=3.50–40.3, $^{87}Sr/^{86}Sr_{(i)}$=0.704–0.705) compared to the lithospheric mantle (SCLM: La/Nb=0.65–1.19, Sr/Y=0.70–18.6, Zr/Y=1.84–3.73, $^{87}Sr/^{86}Sr_{(i)}$=0.704–0.705) and the crust (Precambrian basement metamorphic rocks: La/Nb=1.52–3.33, Sr/Y=5.50–18.6, Zr/Y=3.66–5.37, $^{87}Sr/^{86}Sr_{(i)}$>0.714). With the increasing lithospheric thickness, the influence of the lithosphere increases, resulting in the gradual decrease of the La/Nb, Sr/Y and Zr/Y ratios and the gradual increase of Sr isotopic compositions of melts. In contrast, type-II mafic dikes are derived from the lithospheric mantle without obvious crustal contamination. Therefore, the Sr isotopic compositions, La/Nb, Sr/Y and Zr/Y ratios of these rocks are relatively uniform from the coastal area to the interior and show no correlation to the lithospheric thickness.

4.4 Implications

Previous studies generally suggest that mafic rocks with arc-like trace element geochemistry in southeastern China are originated from a metasomatized lithospheric mantle (e.g., Zhao et al., 2007, 2004; Wang et al., 2003). However, our studies observe the good correlations between Sr isotopic composition, La/Nb, Sr/Y, Zr/Y and lithospheric thickness of type-I rocks, and this phenomenon cannot be explained by previous model. We therefore speculate that these mafic melts were generated by partial melting of the asthenosphere, which contains an amount of subducted crustal materials. During ascent, such melts may have interacted with the overlying lithosphere and their chemical compositions were modified during the interaction. Similar melt-lithosphere interaction has also been observed in the Cenozoic basalts in Northeast China and the South China Sea (Liu et al., 2017, 2016; Zhang et al., 2017). All these observations highlight the importance of lithosphere in the formation of mantle-derived melts, and emphasize the chemical compositions of mafic rocks can be significantly modified during the melt-lithosphere interaction. For this reason, before discussing the genesis of mafic rocks, the potential influence of the melt-lithosphere interaction should be assessed first in the future.

ACKNOWLEDGMENTS

We are grateful to Wenli Xie, Ye Liu, Huanling Lei, Ye He and Xiaoqiu Xue for their technical support. We appreciate the thoughtful and constructive reviews provided by the editors and two anonymous reviewers. This study was financially supported by the National Natural Science Foundation of China (Nos. 41672048, 41802045) and the State Key Laboratory for Mineral Deposits Research, Nanjing University (No. ZZKT-201908). The final publication is available at Springer via https://doi.org/10.1007/s12583-020-1358-y.

Electronic Supplementary Materials: Supplementary materials (Figs. S1–S5, Tables S1–S7, and references cited therein)

are available in the online version of this article at https://doi.org/10.1007/s12583-020-1358-y.

REFERENCES CITED

An, M., Shi, Y., 2006. Lithospheric Thickness of the Chinese Continent. *Physics of the Earth and Planetary Interiors*, 159(3/4): 257–266. https://doi.org/10.1016/j.pepi.2006.08.002

Chauvel, C., Lewin, E., Carpentier, M., et al., 2008. Role of Recycled Oceanic Basalt and Sediment in Generating the Hf-Nd Mantle Array. *Nature Geoscience*, 1(1): 64–67. https://doi.org/10.1038/ngeo.2007.51

Chen, C. H., Lee, C. Y., Shinjo, R., 2008. Was there Jurassic Paleo-Pacific Subduction in South China?: Constraints from $^{40}Ar/^{39}Ar$ Dating, Elemental and Sr-Nd-Pb Isotopic Geochemistry of the Mesozoic Basalts. *Lithos*, 106(1/2): 83–92. https://doi.org/10.1016/j.lithos.2008.06.009

Chen, J. F., Jahn, B. M., 1998. Crustal Evolution of Southeastern China: Nd and Sr Isotopic Evidence. *Tectonophysics*, 284(1/2): 101–133. https://doi.org/10.1016/s0040-1951(97)00186-8

Chen, W. S., Yang, H. C., Wang, X., et al., 2002. Tectonic Setting and Exhumation History of the Pingtan-Dongshan Metamorphic Belt along the Coastal Area, Fujian Province, Southeast China. *Journal of Asian Earth Sciences*, 20(7): 829–840. https://doi.org/10.1016/s1367-9120(01)00066-9

Dai, B. Z., 2007. Geochronology and Geochemistry of the Mesozoic Mafic Magmatisms in Southern Hunan Province, China: Implications for Multi-Stage Lithospheric Extension in South China: [Dissertation]. Nanjing University, Nanjing. 1–141 (in Chinese with English Abstract)

Dasgupta, R., Hirschmann, M. M., Withers, A. C., 2004. Deep Global Cycling of Carbon Constrained by the Solidus of Anhydrous, Carbonated Eclogite under Upper Mantle Conditions. *Earth and Planetary Science Letters*, 227(1/2): 73–85. https://doi.org/10.1016/j.epsl.2004.08.004

Davies, D. R., Rawlinson, N., Iaffaldano, G., et al., 2015. Lithospheric Controls on Magma Composition along Earth's Longest Continental Hotspot Track. *Nature*, 525(7570): 511–514. https://doi.org/10.1038/nature14903

Dong, C. W., Zhou, C., Gu, H. Y., et al., 2011. The Age Difference, Geochemistry and Petrogenesis of Mafic Dikes and Host Granites from Meizhou Island in Fujian Province. *Journal of Jilin University* (*Earth Science Edition*), 41(3): 735–744 (in Chinese with English Abstract)

Fan, Q. C., Liu, R. X., Xie, H. S., et al., 1997. Experimental Study of Spinel-Garnet Phase Transition in Upper Mantle and Its Significance. *Science in China Series D*: *Earth Sciences*, 40(4): 383–389. https://doi.org/10.1007/bf02877569

Feng, M., van der Lee, S., An, M. J., et al., 2010. Lithospheric Thickness, Thinning, Subduction, and Interaction with the Asthenosphere beneath China from the Joint Inversion of Seismic S-Wave Train Fits and Rayleigh-Wave Dispersion Curves. *Lithos*, 120(1/2): 116–130. https://doi.org/10.1016/j.lithos.2009.11.017

Foley, S. F., Barth, M. G., Jenner, G. A., 2000. Rutile/Melt Partition Coefficients for Trace Elements and an Assessment of the Influence of Rutile on the Trace Element Characteristics of Subduction Zone Magmas. *Geochimica et Cosmochimica Acta*, 64(5): 933–938. https://doi.org/10.1016/s0016-7037(99)00355-5

Halliday, A. N., Lee, D. C., Tommasini, S., et al., 1995. Incompatible Trace Elements in OIB and MORB and Source Enrichment in the Sub-Oceanic Mantle. *Earth and Planetary Science Letters*, 133(3/4): 379–395. https://doi.org/10.1016/0012-821x(95)00097-v

He, Z. Y., Xu, X. S., 2012. Petrogenesis of the Late Yanshanian Mantle-Derived Intrusions in Southeastern China: Response to the Geodynamics of Paleo-Pacific Plate Subduction. *Chemical Geology*, 328: 208–221. https://doi.org/10.1016/j.chemgeo.2011.09.014

Herzberg, C., 2011. Identification of Source Lithology in the Hawaiian and Canary Islands: Implications for Origins. *Journal of Petrology*, 52(1): 113–146. https://doi.org/10.1093/petrology/egq075

Hoernle, K., Tilton, G., Le Bas, M. J., et al., 2002. Geochemistry of Oceanic Carbonatites Compared with Continental Carbonatites: Mantle Recycling of Oceanic Crustal Carbonate. *Contributions to Mineralogy and Petrology*, 142(5): 520–542. https://doi.org/10.1007/s004100100308

Hofmann, A. W., 1988. Chemical Differentiation of the Earth: The Relationship between Mantle, Continental Crust, and Oceanic Crust. *Earth and Planetary Science Letters*, 90(3): 297–314. https://doi.org/10.1016/0012-821x(88)90132-x

Humphreys, E. R., Niu, Y. L., 2009. On the Composition of Ocean Island Basalts (OIB): The Effects of Lithospheric Thickness Variation and Mantle Metasomatism. *Lithos*, 112(1/2): 118–136. https://doi.org/10.1016/j.lithos.2009.04.038

Jahn, B. M., 1974. Mesozoic Thermal Events in Southeast China. *Nature*, 248(5448): 480–483. https://doi.org/10.1038/248480a0

Jahn, B. M., Zhou, X. H., Li, J. L., 1990. Formation and Tectonic Evolution of Southeastern China and Taiwan: Isotopic and Geochemical Constraints. *Tectonophysics*, 183(1/2/3/4): 145–160. https://doi.org/10.1016/0040-1951(90)90413-3

Jia, Z. B., Chen, H., Xia, Q. K., et al., 2020. Influence of the Subduction of the Pacific Plate on the Mantle Characteristics of South China: Constraints from the Temporal Geochemical Evolution of the Mesozoic Basalts in the Jitai Basin. *Lithos*, 352/353: 105253. https://doi.org/10.1016/j.lithos.2019.105253

Jochum, K. P., Weis, U., Schwager, B., et al., 2016. Reference Values Following ISO Guidelines for Frequently Requested Rock Reference Materials. *Geostandards and Geoanalytical Research*, 40(3): 333–350. https://doi.org/10.1111/j.1751-908x.2015.00392.x

Le Bas, M. J., Le Maitre, R. W., Streckeisen, A., et al., 1986. A Chemical Classification of Volcanic Rocks Based on the Total Alkali-Silica Diagram. *Journal of Petrology*, 27(3): 745–750. https://doi.org/10.1093/petrology/27.3.745

Lei, H. L., Yang, T., Jiang, S. Y., et al., 2019. A Simple Two-Stage Column Chromatographic Separation Scheme for Strontium, Lead, Neodymium and Hafnium Isotope Analyses in Geological Samples by Thermal Ionization Mass Spectrometry or Multi-Collector Inductively Coupled Plasma Mass Spectrometry. *Journal of Separation Science*, 42(20): 3261–3275. https://doi.org/10.1002/jssc.201900579

Li, Z. X., Li, X. H., 2007. Formation of the 1 300-km-Wide Intracontinental Orogen and Postorogenic Magmatic Province in Mesozoic South China: A Flat-Slab Subduction Model. *Geology*, 35(2): 179–182. https://doi.org/10.1130/g23193a.1

Litasov, K., Ohtani, E., 2010. The Solidus of Carbonated Eclogite in the System CaO-Al_2O_3-MgO-SiO_2-Na_2O-CO_2 to 32 GPa and Carbonatite Liquid in the Deep Mantle. *Earth and Planetary Science Letters*, 295(1/2): 115–126. https://doi.org/10.1016/j.epsl.2010.03.030

Liu, J. Q., Chen, L. H., Wang, X. J., et al., 2017. The Role of Melt-Rock Interaction in the Formation of Quaternary High-MgO Potassic Basalt from the Greater Khingan Range, Northeast China. *Journal of Geophysical Research*: *Solid Earth*, 122(1): 262–280. https://doi.org/10.1002/2016jb013605

Liu, J. Q., Chen, L. H., Zeng, G., et al., 2016. Lithospheric Thickness Controlled Compositional Variations in Potassic Basalts of Northeast China by Melt-Rock Interactions. *Geophysical Research Letters*, 43(6): 2582–2589. https://doi.org/10.1002/2016gl068332

McDonough, W. F., Sun, S. S., 1995. The Composition of the Earth. *Chemical Geology*, 120(3/4): 223–253. https://doi.org/10.1016/0009-2541(94)00140-4

McKenzie, D., O'Nions, R. K., 1991. Partial Melt Distributions from Inversion of Rare Earth Element Concentrations. *Journal of Petrology*, 32(5):

1021–1091. https://doi.org/10.1093/petrology/32.5.1021

Meng, L. F., Li, Z. X., Chen, H. L., et al., 2012. Geochronological and Geochemical Results from Mesozoic Basalts in Southern South China Block Support the Flat-Slab Subduction Model. *Lithos*, 132/133: 127–140. https://doi.org/10.1016/j.lithos.2011.11.022

Niu, Y. L., Collerson, K. D., Batiza, R., et al., 1999. Origin of Enriched-Type Mid-Ocean Ridge Basalt at Ridges Far from Mantle Plumes: The East Pacific Rise at 11°20′N. *Journal of Geophysical Research*: *Solid Earth*, 104(B4): 7067–7087. https://doi.org/10.1029/1998jb900037

Niu, Y. L., Wilson, M., Humphreys, E. R., et al., 2011. The Origin of Intra-Plate Ocean Island Basalts (OIB): The Lid Effect and Its Geodynamic Implications. *Journal of Petrology*, 52(7/8): 1443–1468. https://doi.org/10.1093/petrology/egr030

Pearce, J. A., Peate, D. W., 1995. Tectonic Implications of the Composition of Volcanic Arc Magmas. *Annual Review of Earth and Planetary Sciences*, 23(1): 251–285. https://doi.org/10.1146/annurev.ea.23.050195.001343

Qin, S. C., Fan, W. M., Guo, F., et al., 2010. Petrogenesis of Late Mesozoic Diabase Dikes in Zhejiang-Fujian Provinces: Constraints from Ar-Ar Dating and Geochemistry. *Acta Petrologica Sinica*, 26(11): 3295–3306 (in Chinese with English Abstract)

Shen, X. Z., Kind, R., Huang, Z. C., et al., 2019. Imaging the Mantle Lithosphere below the China Cratons Using S-to-P Converted Waves. *Tectonophysics*, 754: 73–79. https://doi.org/10.1016/j.tecto.2019.02.002

Sobolev, A. V., Hofmann, A. W., Kuzmin, D. V., et al., 2007. The Amount of Recycled Crust in Sources of Mantle-Derived Melts. *Science*, 316(5823): 412–417. https://doi.org/10.1126/science.1138113

Wan, T. F., Tong, Y. F., Zheng, W. W., 1987. Thermal Structure of Lithosphere in Fujian, China. *Geoscience*, 1(3/4): 412–423 (in Chinese with English Abstract)

Wan, Y. S., Liu, D. Y., Xu, M. H., et al., 2007. SHRIMP U-Pb Zircon Geochronology and Geochemistry of Metavolcanic and Metasedimentary Rocks in Northwestern Fujian, Cathaysia Block, China: Tectonic Implications and the Need to Redefine Lithostratigraphic Units. *Gondwana Research*, 12(1/2): 166–183. https://doi.org/10.1016/j.gr.2006.10.016

Wang, X. Y., Yang, Z., Chen, N. S., et al., 2018. Petrogenesis and Ore Genesis of the Late Yanshanian Granites and Associated Porphyry-Skarn W-Mo Deposits from the Yunkai Area of South China: Evidence from the Zircon U-Pb Ages, Hf Isotopes and Sulfide S-Fe Isotopes. *Journal of Earth Science*, 29(4): 939–959. https://doi.org/10.1007/s12583-017-0901-1

Wang, Y. J., Fan, W. M., Guo, F., et al., 2003. Geochemistry of Mesozoic Mafic Rocks Adjacent to the Chenzhou-Linwu Fault, South China: Implications for the Lithospheric Boundary between the Yangtze and Cathaysia Blocks. *International Geology Review*, 45(3): 263–286. https://doi.org/10.2747/0020-6814.45.3.263

Workman, R. K., Hart, S. R., 2005. Major and Trace Element Composition of the Depleted MORB Mantle (DMM). *Earth and Planetary Science Letters*, 231(1/2): 53–72. https://doi.org/10.1016/j.epsl.2004.12.005

Yang, Y. F., 2008. Chronology and Geochemistry of Late Mesozoic Basic-Intermediate Dike Swarms from the Coastland of Fujian Province: [Dissertation]. Zhejiang University, Hangzhou. 1–67 (in Chinese with English Abstract)

Yasuda, A., Fujii, T., Kurita, K., 1994. Melting Phase Relations of an Anhydrous Mid-Ocean Ridge Basalt from 3 to 20 GPa: Implications for the Behavior of Subducted Oceanic Crust in the Mantle. *Journal of Geophysical Research*: *Solid Earth*, 99(B5): 9401–9414. https://doi.org/10.1029/93jb03205

Yu, J. H., Xu, X. S., O'Reilly, S. Y., et al., 2003. Granulite Xenoliths from Cenozoic Basalts in SE China Provide Geochemical Fingerprints to Distinguish Lower Crust Terranes from the North and South China Tectonic Blocks. *Lithos*, 67(1/2): 77–102. https://doi.org/10.1016/s0024-4937(02)00253-0

Zeng, G., Chen, L. H., Hu, S. L., et al., 2013. Genesis of Cenozoic Low-Ca Alkaline Basalts in the Nanjing Basaltic Field, Eastern China: The Case for Mantle Xenolith-Magma Interaction. *Geochemistry*, *Geophysics*, *Geosystems*, 14(5): 1660–1677. https://doi.org/10.1002/ggge.20127

Zeng, G., Chen, L. H., Xu, X. S., et al., 2010. Carbonated Mantle Sources for Cenozoic Intra-Plate Alkaline Basalts in Shandong, North China. *Chemical Geology*, 273(1/2): 35–45. https://doi.org/10.1016/j.chemgeo.2010.02.009

Zeng, G., He, Z. Y., Li, Z., et al., 2016. Geodynamics of Paleo-Pacific Plate Subduction Constrained by the Source Lithologies of Late Mesozoic Basalts in Southeastern China. *Geophysical Research Letters*, 43(19): 10189–10197. https://doi.org/10.1002/2016gl070346

Zhang, B., Guo, F., Zhang, X. B., et al., 2019. Early Cretaceous Subduction of Paleo-Pacific Ocean in the Coastal Region of SE China: Petrological and Geochemical Constraints from the Mafic Intrusions. *Lithos*, 334/335: 8–24. https://doi.org/10.1016/j.lithos.2019.03.010

Zhang, G. L., Chen, L. H., Jackson, M. G., et al., 2017. Evolution of Carbonated Melt to Alkali Basalt in the South China Sea. *Nature Geoscience*, 10(3): 229–235. https://doi.org/10.1038/ngeo2877

Zhang, G. S., 2006. Chronology, Geochemistry, and Geodynamic Significance of the Mafic-Ultramafic Rocks in Fujian Province since Late Mesozoic: [Dissertation]. Institute of Geochemistry, Chinese Academy of Sciences, Guiyang. 1–138 (in Chinese with English Abstract)

Zhang, H. F., Goldstein, S. L., Zhou, X. H., et al., 2008. Evolution of Subcontinental Lithospheric Mantle beneath Eastern China: Re-Os Isotopic Evidence from Mantle Xenoliths in Paleozoic Kimberlites and Mesozoic Basalts. *Contributions to Mineralogy and Petrology*, 155(3): 271–293. https://doi.org/10.1007/s00410-007-0241-5

Zhao, J. H., 2004. Chronology and Geochemistry of Mafic Rocks from Fujian Province: Implications for the Mantle Evolution of SE China since Late Mesozoic: [Dissertation]. Institute of Geochemistry, Chinese Academy of Sciences, Guiyang. 1–116 (in Chinese with English Abstract)

Zhao, J. H., Hu, R. Z., Liu, S., 2004. Geochemistry, Petrogenesis, and Tectonic Significance of Mesozoic Mafic Dikes, Fujian Province, Southeastern China. *International Geology Review*, 46(6): 542–557. https://doi.org/10.2747/0020-6814.46.6.542

Zhao, J. H., Hu, R. Z., Zhou, M. F., et al., 2007. Elemental and Sr-Nd-Pb Isotopic Geochemistry of Mesozoic Mafic Intrusions in Southern Fujian Province, SE China: Implications for Lithospheric Mantle Evolution. *Geological Magazine*, 144(6): 937–952. https://doi.org/10.1017/s0016756807003834

Zhou, X. M., Li, W. X., 2000. Origin of Late Mesozoic Igneous Rocks in Southeastern China: Implications for Lithosphere Subduction and Underplating of Mafic Magmas. *Tectonophysics*, 326(3/4): 269–287. https://doi.org/10.1016/s0040-1951(00)00120-7

Zhou, X. M., Sun, T., Shen, W. Z., et al., 2006. Petrogenesis of Mesozoic Granitoids and Volcanic Rocks in South China: A Response to Tectonic Evolution. *Episodes*, 29(1): 26–33. https://doi.org/10.18814/epiiugs/2006/v29i1/004